International Journal of
INTELLIGENT SYSTEMS AND APPLICATIONS IN ENGINEERING
ISSN:2147-6799 www.ijisae.org Original Research Paper

Ensemble Deep Learning Algorithm for Multi View Image Fusion

Anna Saro Vijendran[1], Kalaivani Ramasamy[*2]

Submitted: 09/10/2023 **Revised**: 30/11/2023 **Accepted**: 09/12/2023

Abstract: In order to create a synthetic image with more valuable data than just single particular image could ever provide, image fusion attempts to combine many image graphs of the similar subject. The clarity of the majority of original images is restricted by imaging sensors' limitations and broadband signal transmission. An innovative multi-modality clinical image fusing technique is presented in this study to enhance the image quality and earlier brain tumor detection performance. Hence, ensemble based deep learning algorithm is proposed in this study to increase the Magnetic Resonance Imaging (MRI) brain image fusion performances by minimizing noises, executing segmentations, extracting features, fusing images in primary phases. Initial noise reduction improves image quality. Segmentation process MRI scans divides an image into its parts. Black-and-white images are created. Following that, Lion Swarm Optimization based Convolutional Neural Network (LSOCNN) extracts image characteristics with most information. Eventually, multi-modal image fusion generated lower, intermediate, and upper level images. It can be seen from all angles and fused. To increase image fusion performance, ensemble CNN, DFMI-Net, TA-cGAN algorithms are presented. From the result, proposed ensemble DCNN+DFMI+Cgan compared to previous methods, this approach performs improved in respect of correctness, clarity, memory, and mean square error (MSE).

Keywords: *Differentiable Fusion with Mutual Information-Network (DFMI-Net), Image fusion, Lion Swarm Optimization based Convolutional Neural Network (LSOCNN), MRI images, Tissue-Aware Conditional Generative Adversarial Network (TA-cGAN).*

1. Introduction

Medical imaging is crucial to clinical diagnostics, surgery guidance, and treatment planning because to the fast growth of sensor and computer science technologies [1]. Irregular cell reproduction causes aberrant brain cell proliferation, which results in solid masses known as brain tumors. They are separated into benign and malignant groups. They are potentially fatal because of how intrusive and persistent they are, which interferes with the brain's regular functions. Furthermore, the edema, or fluid buildup around the tumor, puts stress on normal tissue, causing them to malfunction. Due to radiologists' ability to link swelling to the volume and progression of a tumor, it is crucial in the diagnosing process. The remarkable soft tissue contrast of MRI and CT makes it their more useful modalities for assessing brain malignancies amongst the many brain imaging methods. This study uses an application of an MRI image storage.

Because increasing the clinically diagnostic reliability is the goal of medical image fusion, the resulting fused image must be formed by carefully retaining the most important characteristics and characteristics of the original images. Utilizing either the spatially region or the transformation region to carry out the execution of multifunctional clinical image merging. Through the use of fusing criteria, matching spatial pixels from CT or MRI images merge in the spatial domain [2]. Unfortunately, because to weak edge and contour recognition and distortion, the grade of the combined images is mediocre. The primary issue using spatial domains is that. Because these describe the tumor size or shape, edge and contour representations is often important for clinical image interpretation.

X-ray, CT, and MRI are a few examples of imaging techniques that are often utilized to produce clinical images. These techniques are targeted on revealing data about certain tissues or organs. While CT images assist in precisely identifying solid structures like implants and bones, MRI scans characterize soft tissue in their high-resolution anatomy [3]. The primary goal of image fusing is to create a single complete image encompassing the distinctive qualities of multidimensional clinical imaging, that may assist clinicians in making correct diagnosis across a variety of conditions [4].

In image fusion process, feature extraction is a method of dimension reduction. It is well acknowledged to be a successful method for both lowering computing difficulty and elevating reliability. A powerful method for reducing the dimensions of the information is feature extraction, which is in addition to feature selection. Before projecting a hyperspectral image onto another feature space, a linear transition is used. Following that, only the most important components are maintained for classification [5]. Unsupervised approaches like PCA, ICA, as well as

[1]*Dean-Research, Department of Computer Application, Sri Ramakrishna College of Arts & Science, Coimbatore, Tamil Nadu, India.*
Email: saroviji@rediffmail.com
[2]*Research Scholar, Department of Computer Science, Sri Ramakrishna College of Arts & Science, Coimbatore, Tamil Nadu, India.*
** Corresponding Author Email: tokalai.2011@gmail.com*

monitored methods like linear classifier evaluation, have been used to reduce dimensionality. These strategies are examples of dimensional space reducing methods. Principal component analysis (PCA) is an approach with the capability of maintaining majority of hyperspectral image information using very small numbers of important principal components (PCs).

In current era, many feature selection approaches are utilized on medical database to extract most relevant data. These selection techniques are performed on medical data for various disease prediction. In attempt to simplify things and make computations less difficult, Heuristic and evolutionary strategies are used in most feature selection methods. High-dimensional optimisation issues may be solved with acceptable results and time using such approaches [6]. The most widely used meta-heuristic approaches inspired by nature are those using swarm-based algorithms. One AI-based technology called SI (swarm intelligence) offers aggregate behaviors for autonomous and distributed devices. There are basic actors living there who solely interact with one other and their immediate surroundings regionally.

The goal of an image fusion system that integrates the curvelet transformation with fuzzy statistics is to enhance the depiction of anatomical and pathological data of malignant brain tumors. The primary focus of the fusing procedure is the tumor and the hyper-intense area around it, which enhances radiologists' access to brain imaging information. Some components of this established technique include curvelet transformations, fuzzy entropies, and region-based fuzzy energies [7]. Here, two fusion rules combine lower- and higher-frequency image sub bands.

This study aims to robustly merge MRI images. Several research and methods exist, however neither early brain tumor detection nor considerably improved image clarity have been attained. This study suggests the extended DCNN+DFMI+cGAN schema to overcome the aforementioned problems and enhance the efficiency of systems. The primary result of this study is noise removal via AMF, segmentation using RGKMC, feature extraction using LSOCNN algorithm, and image fusion using ensemble deep learning algorithm. The recommended method improves reliability by using efficient algorithms for the available MRI image database.

This task will be organized as follows for the remainder: Section 2 is going to detail the research study for the segmentation based image fusing systems. Section 3 is going to discuss the results of this study. In the next section, "Section 3," a detailed presentation of the suggested image fusion approach is given. In Section 4, we will discuss the findings of the experiment. The work is summarized in Section 5, which is the last section.

2. Related Work

Subbiah Parvathy et al. [8] suggested innovative fusion approach based on deep learning principles and optimum thresholding. In the shear let transform, the ideal threshold for the fusion rules is chosen using an Enhanced Monarch Butterfly Optimization (EMBO). Subsequently, lower and higher frequency sub-bands obtained were merged from extracted feature maps using deep learning. In this case, the MMIF technique is carried out using the Restricted Boltzmann Machine (RBM). For validation and learning, a reference database was used. Utilizing a collection of frequently used, publically available pre-enrolled CT and MR images, the studies were carried out. The fused image is attainable via the use of fused low level frequency groups in conjunction with high level frequency groupings. The expected outcomes of the model were achieved and it was demonstrated that the model provided efficient achievements in terms of standard deviations (SD), edge qualities (EQ), mutual information (MI), fusion factors (FF), entropies, correlation factors (CF), and spatial frequencies (SF) with their respective values.

Hsu et al. [9] introduced region-based image fusion is a technique that replaces individual pixels with just one other pixel at a time. This approach incorporates characteristics of both feature and pixel-level fusion methods. The fundamental concept is to perform segmentation solely on the far-infrared image, and then to add information about each area from the segmented image to the visible image in appropriate order. Then, in accordance with each area, we determine several fused parameters. Finally, as there is a nonlinear connection between fused parameters and image attributes, we apply artificial neural networks to address the issues of changing time or weather. It allows automated production of fused parameters. The approach has strong adaptable capability with automated fused parameters, according to testing data.

Liu et al. [10] suggested a deep CNN model for mapping encodes. This proposal solves the problem of current fusion techniques by combining generating the activities level assessment and fusing rules by training a CNN model. This work used a novel multi-focus image fusions based on aforementioned concepts. According to testing findings, the approach can achieve cutting-edge merging efficiency in perspective of both visual quality and objective evaluation. Real-world applications may use parallel computing. The learning CNN model is briefly applied to other image fusion issues in the tests.

Yan et al. [11] observed that multi-view approaches may successfully maintain the integrity of data despite their inherent diversity. As a result, we make an effort to bring

the hash learning field using the multi-view deep neural network and create a retrieval model that is both effective and cutting-edge. This model resulted in considerable increases in its ability to retrieve information. Their usage of neural networks in a supervised multi-view hash model, enhanced multiple views of the data. It integrates multi-view and deep learning techniques to create a brand-new hash learning approach. The suggested technique constantly explores the relationships between aspects, that would impact the network's overall optimizing strategy, using an efficient view stability assessment approach. To maintain the benefits of both convolutional and multi-view, a variety of multi-data fusion techniques must be developed in the hamming area.

Ma et al. [12] suggested DDcGAN, a special front-end model for combining images from visible and infrared spectrums at various resolutions. This strategy developed a game fostering discriminations with the objective to produce merged images that appear nearly like the originals. The objective of the classifier was to identify information losses, any structural distinctions that exist amongst two source images and fused image. The combined image must maintain both thermal radiation and texture data. In order to match the infrared image, DDcGAN restricts the down sampled merged image when combining source images using varying resolutions resulting in preserving structural details and without distorting thermal radiation data. DDcGAN was used to combine high-resolution magnetic resonance images with low-resolution positron emission tomography images. DDcGAN outperformed other techniques in terms of visual impacts and quantitative metrics both in statistical and qualitative tests on accessible datasets.

Zhang et al. [13] presented generative adversarial networks that fused multi-focus images using gradient-joined join constraints. To determine source pixel focus based on recurring blur difference, an effective selection block is implemented in this model. When correctly created, content losses may be utilised to dynamically regulate bias in optimizations, and generators provide synthetic outputs with the same dispersion as the desired source frames. Gradient maps of combined outputs relate to global gradient maps formed from source pictures in a conflicting game. This allows for the texture details to be improved even more. This model does not need any ground-truth fused images in order to be trained. A fresh database with 120 excellent multi-focus image pairings is also made available for benchmark testing. In respect of both the objective visual effect and the quantitative metrics, testing findings show that the procedure is better to the state-of-the-art.

3. Proposed Methodology

A group deep learning approach is suggested in this study to considerably enhance the efficiency of image fusing. Fig. 1 displays the recommended technology's overall block diagram.

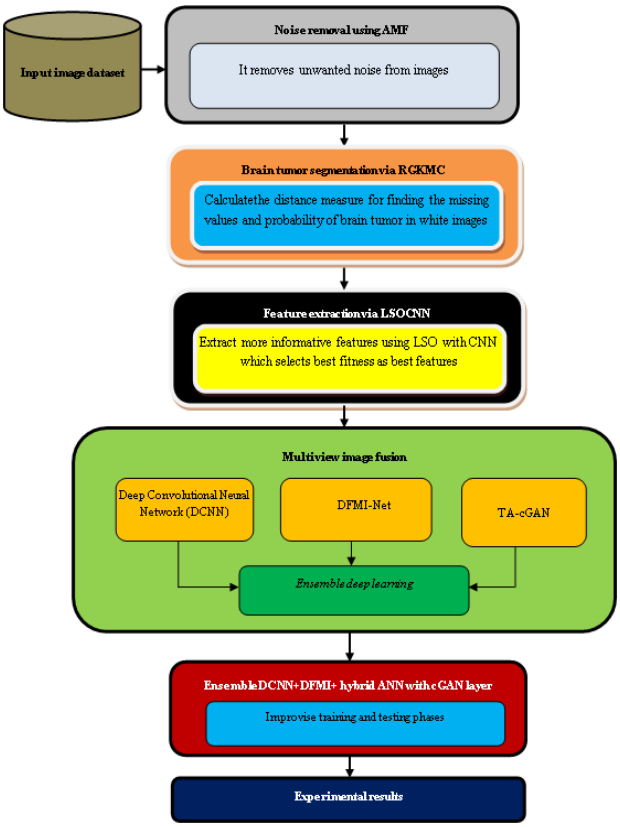

Fig. 1. Flowchart of the Suggested Architecture

3.1. Input Image Dataset

Using four different MRI modalities for each patient, the BraTS 2018 dataset provides multi-modal 3D brain MRIs and separations of brain cancers analyzed by medical practitioners (T1, T1c, T2, and FLAIR). Three tumour subregions have been identified in the observations: the necrotic, expanding tumour core, the peritumoral edoema, and the enlarging tumor. The findings are divided into three nested sub-regions, including overall tumour, central tumour, and enhancing tumour. Using various MRI scanners, the data was compiled from 19 institutions.

Noise Removal using Adaptive Median Filtering (AMF)

AMF algorithm removes unwanted noise from images in this work. Its primary purpose is to improve image quality in high-noise environments. For the purpose of identifying the pixels in a image that has being impacted by distortion, AMF conducts spatially analysis [14]. Each pixel in the image is evaluated in relation to its immediate neighbors by the AMF before being classified as noisy. Variable parameters include the neighborhood's size and the matching criterion [15]. If a pixel differs from most of its neighbours and does not share a structural alignment with pixels that are similar in other ways, it is noisy. After that, the median pixel value of the surrounding neighborhood's noise-free pixels is used to replace these noisy pixels. Noise labeltests determine noise-free neighborhood pixels. Hence, it reduces image noise to improve image clarity.

The adaptive filter's window size is adjusted in response to the number of noise sources that may be present in a particular area. The window size in each region is determined by counting the noisy pixels (1). The mean square error (MSE) parameters for adjusting the window size based on the amount of noisy pixels in a region are calculated after thorough computations to provide the optimum outcomes.

$$W\,(M) = \sum_{p} C(p, D_P) + \sum_{q \epsilon N_p} T\left[\left|M_P - M_q\right| = 1\right] + \sum_{q \epsilon N_p} T\left[\left|M_P - M_q\right| > 1\right] \quad (1)$$

The best solution of W is M. The actual pixels in images are p, and q signify neighbors. Pixels next top are marked as N_P. The estimated matched windows of p and q are denoted by $M_P and M_q$ respectively. A specific matching window's cost is indicated by the letter C. $T[\cdot]$ is a logical function that examines the assertions it contains, determines whether or not those statements are true, and then either returns 1 or 0. In the above equation (1), extend the size of the window if there is not a single pixel in the window that is devoid of noise, or if the median pixel in the window contains noise. The adaptive nature of the window size utilized to filter the image pixels causes it to grow if the predetermined requirements are not satisfied. The pixel is sorted using the window's median if the requirement is satisfied. Let $I_{ij}$is the pixel that makes up the image that has been messed up, I_{min}be the least amount of pixels possible, I_{max}be equal to the pixel value that is its highest possible in the window, Wrepresent the size of the window that is currently active, W_{max}be the largest achievable window size, and I_{med}represent the middle point of the given window. There are two levels for this filtering technique algorithm, as given below.

Level A:

a) If $I_{min} < I_{med} < I_{max}$, then it implies the median values are noise-free. Hence, Level B assesses if the current pixel is noisy.

b) In the event that this is not the case, the window size is increased using equation (1), and when maximum window sizes are reached, the model switches to Level B until median values are no longer noisy; otherwise, median values are utilized as the pixel values for filtered images.

Level B:

a) If $I_{min} < I_{ij} < I_{max}$then the present pixel value is not affected by noise, and as a result, the filtered image always has the same pixel.

b) In the alternative, if the value of the image pixel is alternatively equivalent to $I_{max} or I_{min}$(corrupted), subsequently the filtered image Level A's median value is assigned to pixel.

Brain Tumor Segmentation via Region Growing based K-Means Clustering (RGKMC) Algorithm

RGKMC algorithm effectively segments brain tumours in this study. Brain tumour segments distinguish tumours from normal brain tissue, aiding diagnosis and treatment. Owing of tumours' irregular form and imprecise limitations, it's still tough. In this study, RGKMC algorithm is presented to solve the issue.KMC is a useful grouping method that separates data into categories depending on the initial grouping centers of groupings [16]. KMC is utilized to accomplish this task. In order to determine where the groups' centers are located, it applies the Euclidian metric. Images are segmented by RGKMC. This research detects brain tumours in both images. The process computes current cluster centres and reassigns data pieces to clusters with closest centres. Once all reevaluations have been made, it comes to an end. This technique locally minimizes the based on inter variability, which is the sum of the squares of the discrepancies among the information characteristics and the group center that

correspond to them. Fig. 2 shows the example of KMC algorithm.

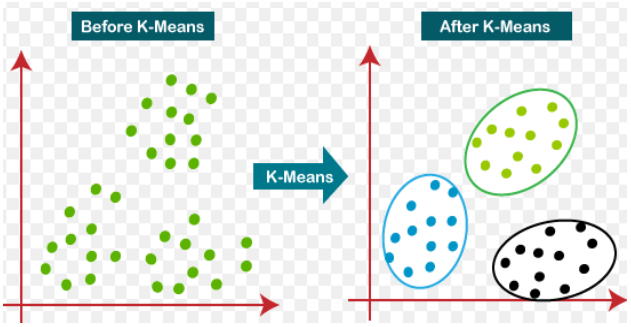

Fig. 2. Example of KMC Algorithm

Due to the fact that starting seed points are chosen, it is categorized as a pixel-based image segmented procedure. Using starting seeding points as a starting point, this segmented method looks at the surrounding pixels to see whether they must be included in the segmented area. Recursive techniques include regional splits and regional combining. To create a suitable segmented image of the original image, areas are often first combined to break an image into highest number of areas [17] which asserts that adjacent pixels located into identical areas had comparable intensity levels.

Advantages of K-means include straightforward executions and linear runtimes with respect to the amount of items. The number of clusters is maintained in this work at one per category. Applying the formula provided here, determine the Euclidean distance to determine the group vertices.

$$d(i,j) = \sqrt{\sum_{i=1}^{n}(x_i - y_i)^2} \quad (2)$$

When two points in Euclidean n-space are denoted by x_i and y_i respectively

Algorithm 1: RGKMC Algorithm

1. Pick an amount of groups, k, from the available options MRI database (D)
2. Group centers should be established µ1,…µk and segment black & white images
3. Set clustered centroid to such locations using k data pointsfor extracting starting seeds
4. Give group points at random, then compute group meansand find neighboring pixels
5. Determine the group centers that every information point is most closely associated with, as well as the distance measure that will be used to determine which values are missing (2)
6. Examine region growing pixels using (2) and select minimum distanced pixels
7. Check similarities between pixels and update closest existing regions that are connected to seeds and attach this group to data points.
8. Recalculate group centers and find the tumor in black images
9. Identify the earlier prediction probability of brain tumor in white images
10. Once there have been no fresh reevaluations, stop.

RGKMC The whole database is used to create clusters of complete pixels. One pixel at a time fills region-based pixels with their prospective values. With black-and-white images, it detects brain tumours early. Based on tumour markings, it splits black-and-white images. In this study, RGKMC algorithm evaluated white images' earlier likeliness of tumours. As a consequence of applying RGKMC to MRI database groups, freshly inserted pixels are examined for their correct class grouping and if so, the numbers are rendered permanent, and process repeated for subsequent pixels and for pixels located in incorrect groups, next potential numbers are provided and matched until their locations are determined. At this study, the RGKMC approach is also employed to raise the image categorization efficiency in higher resolutions, which increases the efficiency of early brain tumor detections.

Feature Extraction using Lion Swarm Optimization based Convolutional Neural Network (LSOCNN)

In this study, LSOCNN algorithm extracts more useful features utilising optimum fitness values. Three convolutional layers mine image attributes from source images in feature extraction. Image fusion relies more on feature mining.

CNN's optimal method is efficient initialization and convolution kernel training. Thus, employ GoogLeNet's convolutional layer. In ImageNet, the primary Convolutional Layer (CONV1) has 64 convolution cores of 7 × 7 dimension to extract an image's efficient features.CONV1 has a wide recognition range, but more illustrations may be employed. Hence, fusion need not display all image properties. The second and third Convolutional Layers screen CONV1 characteristics and provide an attribute plot that may be merged. If input images are improperly sampled, image data may be lost. Such missing data might impair feature extraction results. Change the kernel constant speed and padding of each convolutional layer.

Lion Swarm Optimization (LSO) algorithm is metaheuristic, and each iteration of the algorithm might provide many answers. The biggest and toughest animal,

the lion, lives in packs with resident females. Lions and cubs protect the place where they socialize or call home [18]. The territorial lion challenges a traveling Lion to a duel, and the winner retains that status while driving the loser out. The territorial lion's pups are also slain if the traveler wins, and the female is forced to mate under duress. Additionally, as they reach adolescence, cubs confront the lion for retaining control of the area.

Where these behaviors occur, lions' social behavior might be either migratory or residential. Depending on lions' social behavior, which might take the form of acquisition or defensive, LSO seeks to find the best possible solution to challenges. Fig. 3 depicts the characteristics of LSO.

- Territorial Defense: Local lions and cubs engage in combat with itinerant males to control area. LSO compares a new solution against the existing one for evaluation. The territorial lion or current option is replaced if the nomad is superior.
- Territorial Takeover: In addition to deleting any current options, LSO exhibits this characteristic by only storing the finest male and female remedies.

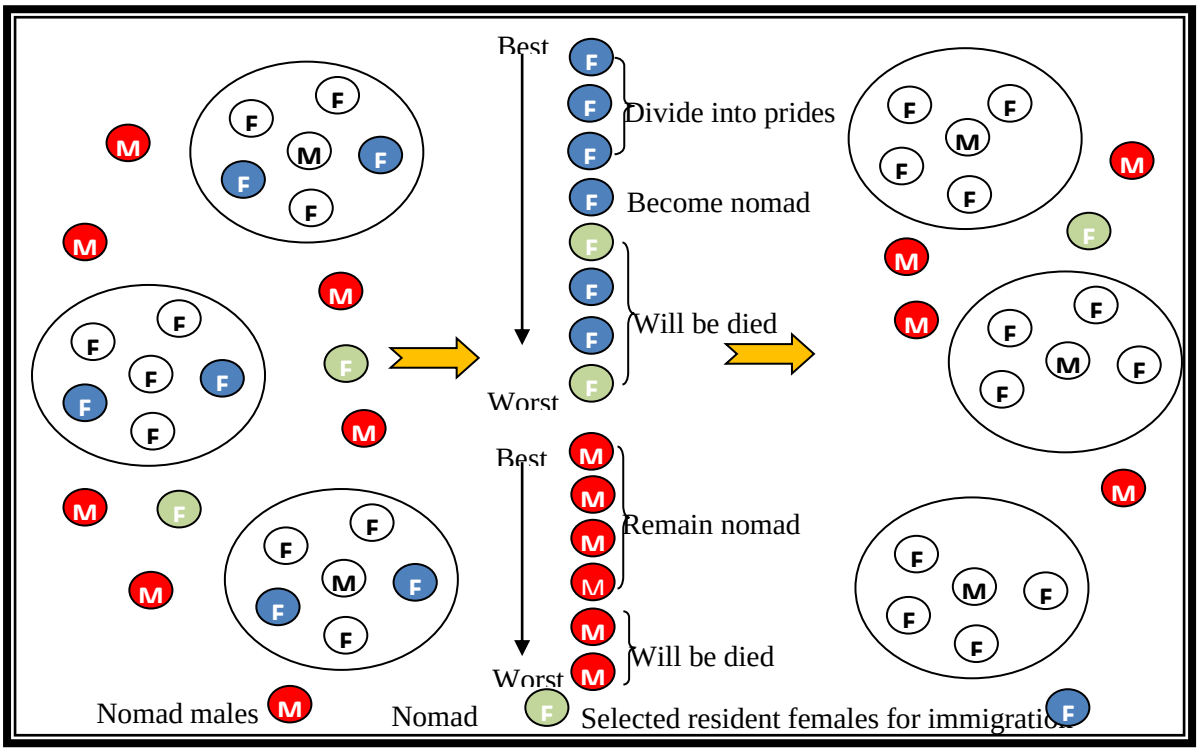

Fig. 3. Nature of LSO

Initialization: LSO The random creation of the lion population is the first step in the initiation process. This population is then saved in matrix form as the remedy space. Lions are remedies that are defined by:

$$Lion = [x_1, x_2, \ldots . x_{N_{var}}] \quad (3)$$

Where $x_{N_{var}}$ are the generic image pixels selected. The proportion of nomadic lions that are created at random is represented by N, while the remaining lions are residents. LSO, which is capable of searching for and identifying hidden connections between the various parts of a network, is used to carry out the solution that is necessary for picking the pixels from the inputs.

Fitness Computations

The relative merits of individual lions in the sorted and stored matrix are subjected to an empirical evaluation.

$$f(Lion) = f(x_1, x_2, \ldots . x_{N_{var}}) \quad (4)$$

Fitness values are based on higher classification accuracy. Most required parameters for this fitness function involves higher accuracy given in

$$Fitness = Max \frac{\sum_{i=1}^{N} (P^i_{neighborhood\ pixel\ with\ higher\ accuracy} + P^i_{quality\ pixels})}{2} \quad (5)$$

$P^i_{neighborhood\ pixel\ with\ higher\ accuracy}$–closer neighborhood pixels and $P^i_{quality\ pixels}$–quality image pixels

During the process of calculating fitness values, these solutions are given an update since they are the activities that are employed. These operations include hunting, mating, wandering, and defense. Because female lions only hunt for food inside their own territory, this means that the area itself is the best place to look for a meal. The values of the fitness function stated earlier are used, together with

future updates, to guide the selection of features to extract in this particular piece of work.

Hunting operation: Hunters are divided into three groups. Although the remaining two hunters make up its left and right, the central hunter has the greatest fitness value. When a hunter's strength increases and their position is upgraded, they arbitrarily choose hunts to assault mock preys who then flee.

Movements towards safety: The rest of the female lions wait in areas of safety while a few of them search for prey. Calculated and stored are the ideal places for each region. The lions have strayed from the ideal spot, as indicated by a high win count. Lower values show that lions are searching for improvement, and competition evaluations show accomplishments as a result.

Roaming of Lions**:** The functioning of roaming is challenging and limits lion searching. This is used by LSO to explore a searched space and locate a better solution. In order to reach their chosen region, lions migrate by n units.

$$n \sim U(0,2 * d)$$

A male lion's distance from a chosen area is indicated by the number d, where n is a random integer with uniform distributions. In the search area, nomadic lions also roam at random.

Mating: The process of breeding and a lion's ability to survive depends heavily on mating. Lion babies are born after selecting the best male and female lions. Crossovers and mutations were used in this procedure to create the greatest and newest solutions from the current ones. The best solutions are obtained by eliminating the weak lions.

Defense: Lions place value on this behavior. A fight between lions occurs between mature males. Following a conflict, a nomadic lion that prevails takes over the defeated animal's domain. In order to protect the lions from newly mated local males and itinerant males, the LSO employs two different defensive strategies. LSO discovers the group's savviest lion as a result.

Migration: This procedure involves moving arbitrarily selected females to new locations, after which the finest females take the places of the normalized females, according to fitness values.

Population equilibrium of Lions: An equilibrium point or position of stability in the lion population is reached at the conclusion of each cycle. At this moment, a count for the maximum number of lions of each gender is determined. The number of lions has been reduced through the removal of those with poor fitness scores.

Criteria for Termination: When additional iterations provide the best fitness values, the suggested method ends. The optimal strategy is to extract the feature with the greatest fitness values, which is then used to improve both image merging efficiency and categorization correctness. Lions with lower fitness values are continually being replaced with lions with better fitness values as part of the territorial takeover operation. As a result, only the solutions that include both males and females are kept, while the rest are eliminated.

Algorithm 1: LSOCNN

Input: MRI image features

Output: More informative features

1. Begin the algorithm
2. Arrange Database
3. It is crucial to consider all the characteristics while selecting the database to administer and categorize samples for CNN during this phase.
4. Objective function (x), $x = (x1,...,)T$ consider lower MSE, execution time and higher accuracy as objective functions
5. Initialize the lions and the random position
6. Set CNN representations, with factor obtained by LSO (convolution layers' quantity, filter dimensions, quantity of convolution filters, and batch dimensions). The CNN is set in combination with extra factors for equipping CNN to mound inputs.
7. CNN preparation and validation - CNN examines images in the input database for preparation, validation, and testing; this process results certain degrees of recognition.
8. Estimate the objective function. The LSO procedure calculates the objective function to conclude the best value
9. Evaluate the fitness of each feature using (5)
10. Select the initial feature and compare with each features to check the quality
11. Select the best image feature pixels which has higher accuracy and lower MSE & execution time
12. Memorize the best image pixels
13. For each feature do
14. Find the best solutions
15. End for
16. Update the position of feature and best feature
17. Merge new best feature and old best feature
18. Sort all the features according to their fitness

19. Discard weaker feature and remained feature become optimal
20. If the requirements for termination are met,
21. Select the top feature set and provide it set
22. Else
23. t=t+1
24. Until t > Max_Iteration
25. Return the optimal image features
26. Lastly, the optimum resolution is designated. In this process, the lions select optimum feature for the CNN model
27. Stop the algorithm

The above listed LSO is described in algorithm 1; in conclusion The largest and most socially active animals, lions, engage in both sedentary and mobile social activity. These two behaviors are alternated by lions. The region is home to resident lions, who breed there to produce young. Movements of nomadic lions are intermittent, with the outclassed males moving in pairs or alone.

Image Fusion of Multi Modal Image

The goal of image fusion is to maintain the information that is complimentary to one another while getting rid of the redundant information and distortion that is present in each of the separate source images. Measures of performance are thus very necessary in order to evaluate how successful the fusion process is and to evaluate and contrast the outcomes of the various algorithms. It is essential to the process of diagnosing and treating brain cancer to have an accurate assessment of the tumor's nature as well as its dimensions, location, and degree of dissemination. Fused MRI brain images can diagnose brain malignancies quicker. They outperform MRI images. Telemedicine's remote diagnosis and speedier first aid are transforming several healthcare areas [16]. Extraction of features is a broad phrase for producing variables pairings to solve these challenges and accurately describe the data.

DCNN Algorithm

Using four independent mammography images from each patient, a deep convolutional neural network model was trained. This approach has been developed using the mini-MIAS and CBIS-DDSM databases, which are curated breast imaging subsets of DDSM. From four mammography representations, the CNN model extracts a variety of characteristics. Early fusion is used during the training process to get data from many perspectives. The process of combining many feature vectors into one feature vector is known as initial fusing. Two methodologies make up the CADx system's four-views features fusion foundation [19].

Before taking into discussion such a network, significant tests with various adjustments in the hyper - parameters are conducted. To choose the optimum categorization networks, we carried out the following hyper parameter modifications.

1. We varied the number of convolution layers from 3 to 7 layers during the first step of feature extraction. Following all convolutional layers, the empirical assessment additionally utilizes maximum and average pooling.
2. Convolutional layers and the last two fully integrated layers are used to assess two activating functions, namely ReLU and Leaky ReLU. The final categorization layer tests the sigmoid and softmax functions.
3. The optimization approach stochastic gradient descent is evaluated with various starting learning rates ranging from 1e-2 to 1e-5. The momentum value is adjusted from 0.7 to 0.9.
4. The ratio among 15% and 50% is used to measure the dispersion after various convolutions and fully linked layers are assessed.

Input and output layers, as well as a number of hidden layers, make up the fundamental DCNN. Convolutional, pooling, and fully linked layers are the most common types of hidden layers in DCNNs. Convolution layers must perform convolutions on inputs before transmitting outcomes to subsequent layers. Convolutions are used to mimic neurons' responses to visual inputs. Convolution networks local or global pooling layers combine groups of neuron outputs into one neuron in following layers. Mean pooling averages the preceding layer's neuron clusters. Fully linked layers link all neurons in one layer to those in another. In its fundamental structure, a deep convolutional neural network (DCNN) is analogous to conventional multi-layer perceptron neural networks. Deep Convolution Neural Networks encompass input, convolution, and classification layers. When it comes to evaluating data with a large number of dimensions, this technique offers a number of clear benefits. A parameter sharing system, which is employed in convolutional layers to regulate and minimize the number of parameters, is implemented by it.

Differentiable Fusion with Mutual Information-Network (DFMI-Net)

The auto encoder structure follows the Fusion W-Net (FW-Net) [20]. The U-Net [21], which produces a visually fused image by aligning the output vectors via a local connection structure, is the foundation of the FW-Net. Additionally, FW-Net can extract semantic data from source images, which are often conveyed by differences in brightness, and

then map semantics of source images from various viewpoints to same semantic spaces. Important characteristics for diagnosis are also located in similar areas simultaneously with structural/edge data and other details. The encoder $E\phi$ provides fused images of same sizes as source images after receiving two geographically and temporally coordinated images. The decoder $D\varphi$ assembles two rebuilt images from merged images after their receipt. In general, the lossfunction is:

$$Loss = \sum_{n=1}^{N} [\alpha_n . \mathbb{E}[|x_n - \widehat{x_n}|] + \beta_n . MINE(x_n, x_f)] \quad (6)$$

Where $x_n$indicates the incoming images, $\widehat{x_n}$the related recovered images are indicated by, and *xf*the merged image is indicated. The first term in equation (6) stands for mean absolute error (MAE) loss, which computes pixel losses of input images and reconstructed images. By minimising MAE losses, encoders keep key elements of source images in fused images [22]. The second component of Equation (5), sometimes referred to as MI losses are representations of common data between input images and synthetic images as determined by MINE-Net. A better fused image is created by increasing the Mutual Information (MI) loss.

Tissue-Aware Conditional Generative Adversarial Network (TA-cGAN)

The TA-cGAN Additionally, it is made up of two auxiliary networks, which are referred to as the generator and the discriminator. On the other hand, in contrast to the original GAN, which is primarily used for the translation of one image into another, the new GAN is able to: TA-cGANis intended for the translation of images into other images; that is, it accepts several images as input and produces a single fused image as output. The following is a full explanation of the network architectures used by the TA-cGAN:

Generator

The generator was created with a U-Net based methodology. Using a skip-connection method, U-Net combines low-level features from shallow encoding layers with high-level characteristics from deep decoding levels. Additionally, the skip connection approach can be used to partially resolve the issue of vanishing gradients. The hop connection concept has been successfully applied to U-Net for a variety of imaging applications, including image synthesis [23]. The network design of the G generator in this study is made up of the encoder and decoder, as shown in Fig. 4. The starting points are the MRI IM picture, the matching label map IL, and the PET IP image. get online. The network's output is the combined IF image. Fig. 4 illustrates the 12 convolutional layers that make up the entire generator network. Six downsampling layers employing batch normalisation (BN) and rectified linear unit (ReLU) operations are included in the encoder component. with convolution and a stride of two. Notably, we do not employ a pooling operation because doing so would reduce the feature map's spatial resolution and prevent the network from detecting minute features in MRI images. The major reason we don't utilise it is because of this. Additionally, each layer of down sampling employs 1x1 zero padding. Six sample levels make up the decoding portion; the final layer only performs convolution operations using a 1x1 filter, whereas the previous five layers carry out convolution-BN-ReLU operations. The decoding part uses skip connections to combine the encoder and decoder layer feature maps. Fig. 4 illustrates the 12 convolution layers that make up the entire generator network. Six downsampling layers employing batch normalisation (BN) and rectified linear unit (ReLU) operations are included in the encoder component. with convolution and a stride of two. Notably, we do not employ a pooling operation because doing so would reduce the feature map's spatial resolution and prevent the network from detecting minute features in MRI images. The major reason we don't utilise it is because of this. Additionally, each layer of down sampling employs 1x1 zero padding. Six sample levels make up the decoding portion; the final layer only performs convolution operations using a 1x1 filter, whereas the previous five layers carry out convolution-BN-ReLU operations. The decoding part uses skip connections to combine the encoder and decoder layer feature maps.

Discriminator

The convolutional D, in contrast to the generating G, is primarily intended to address the categorization issue. Distinguishing fused image pairs from MRI image pairs are particularly the main objective of determiners D in this work. The network topology of the classifier D employed in the investigation is shown in Fig 5 [24] [25]. As shown in Fig. 5, the convolutional D's inputs are either the fused image pair or the MRI image pair, and the network's output is the class label, which indicates whether or not the image pair is differentiated.

Ensemble Deep Learning

In this section, DCNN, DFMI-Net and TA-cGAN algorithms are ensemble to improve the multi view image fusion performance. GAN algorithm is fine-tuned by using ANN algorithm. Fig. 5 is an illustration that provides a high-level overview of the discriminator's general design. Discriminator D uses a straightforward convolution neural network as its network architecture. This has five convolution layers, including one fully linked layer, and sigmoid activation function. The convolution is carried out by the convolutional layers that are located above, which are structured similarly to the encoder that is located in the

generator G. BN-ReLU business and operational issues.

Assisted adversarial network is employed for integrating PET and MRI images. This integrations is viewed as a competitive game between classifier, generator and two agents. The tissue label maps created from MRI images are essential to both of these players. As a result, the game is for two players. High spatial resolution, detailed structural data regarding soft tissues, and colour data indicating the functional properties of the tissue are all provided by the MRI technology. It is a technique for merging brain scans that helps medical professionals make more accurate diagnoses of disorders. MRI images generated with the TA-cGAN approach.

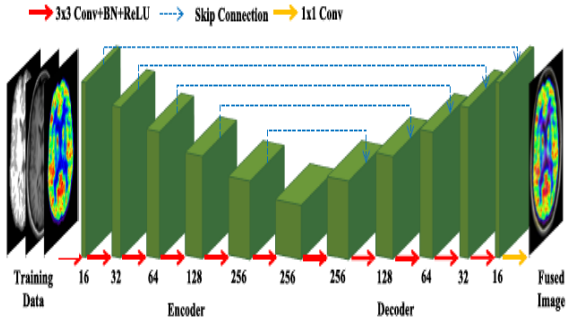

Fig. 4. Network Architecture of the Generator

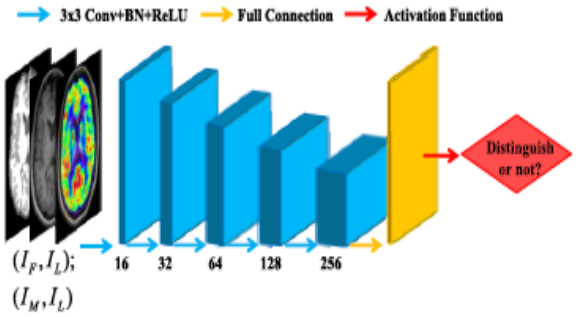

Fig. 5. Network Architecture of the Discriminator

Utilizing learning, ANN is used to gather knowledge. The input layer, hidden layer, and output layer of an ANN are each divided into three phases. A layer known as the input layer gathers input images, processes them, and produces an infinite number of inputs. Various weights are used to guide these operations. In order to address issues in neural networks, weights provide information [26]. After some helpful hidden extraction, a hidden layer takes data that was previously concealed from the input layer and transfers it to the output layer. To identify high-quality image characteristics in this case, ANN is utilized. Classification of state characteristics is performed after utilizing ANN to train the database of MRI images [27-31].

Training of the Discriminators

Every Tepochs, for a fixed $\boldsymbol{\varphi}$, the generator generates $2n$batches $\{B_{a1}, \ldots, B_{an}, B_{g1}, \ldots, B_{gn}\}$quality points that are not obtained from the real datasets that are equal to b pixel points. In addition to this, the discriminator uses a batch for each database i that is sampled.Bripoints from the database that is accessible to it Di. Every single batch that is created is sent by the generator$Bai$to every database $i$which, in turn, generates the loss value shown in the next paragraph:

$$L_i(\theta_i) = \frac{1}{b}[\sum_{x \epsilon B_{ri}} \log D_{\theta_i}(x) + \sum_{x \epsilon B_{ai}} \log(1 - D_{\theta_i}(x))] \quad (7)$$

$L_i(\theta_i)$describes an estimate of every database discriminator's values functional (1). The database adjusts its weights using a gradient descent algorithm like the Adam optimizerθ_i

Training of the Central Generator

Every T epoch, every database i uses $B_{gi}$to calculate the following loss:

$$L_i^g = \frac{1}{b}[\sum_{x \epsilon B_{g_i}} \log(1 - D_{\theta_i}(x))] \quad (8)$$

It roughly represents every dataset generator's values method in (8).

TA-cGAN uses spectral loss as well as joint losses L_{Spec}, structural loss L_{Str} and adversarial loss L_{Adv}. The following is how the joint loss employed in the study is stated mathematically:

$$L_{joint} = \lambda_1 L_{Spec} + \lambda_2 L_{Str} + \lambda_3 L_{Adv} \quad (9)$$

when spectral loss occurs L_{Spec}demands that identical color information be included in the merged image; Loss of structureL_{Str}tries to replicate the structural data in the MRI image in the merged image; Loss of conflictL_{Adv}seeks to enhance the merged image with additional data; $\lambda_1, \lambda_{2\ and}\ \lambda_3$spectrum, behavioural, and aggressive loss values.

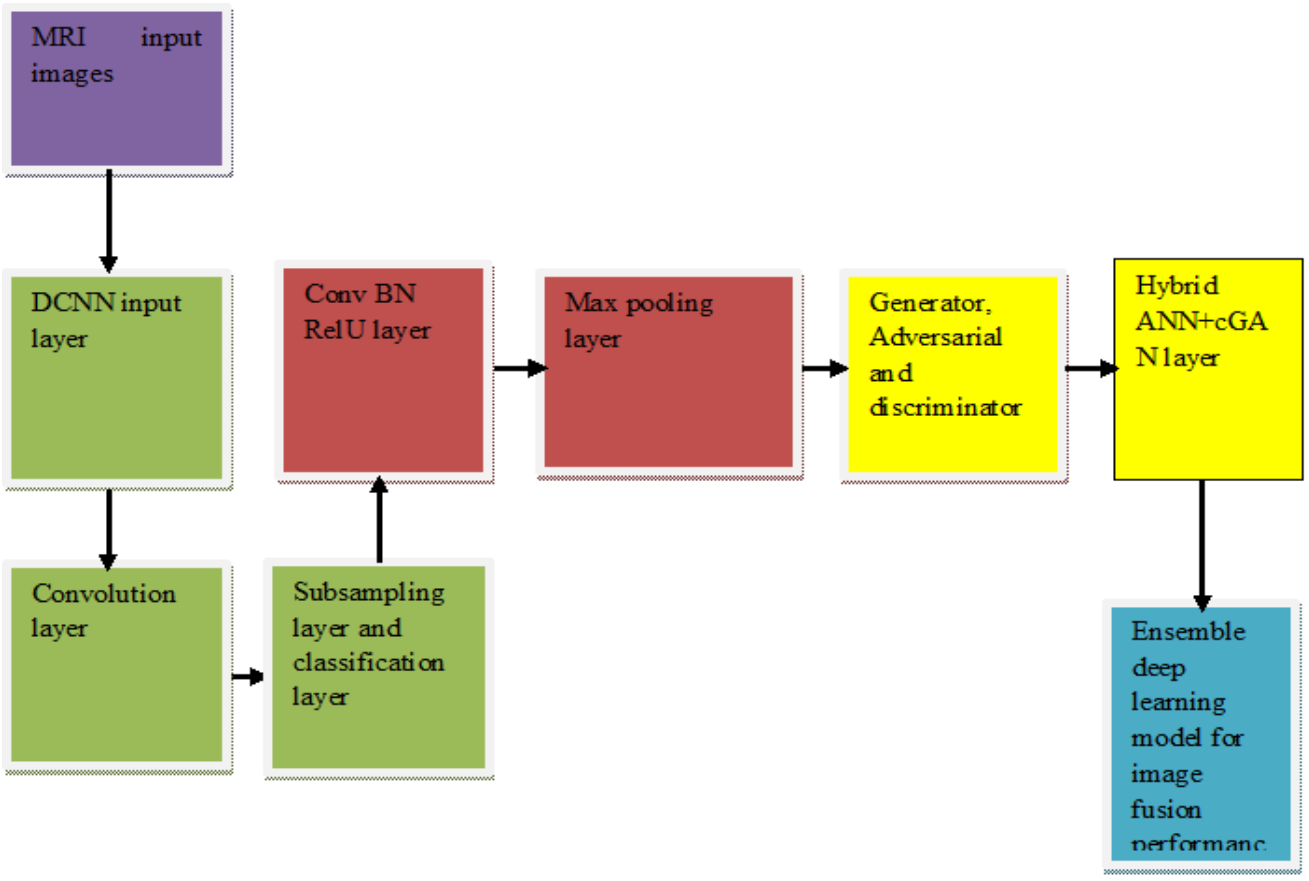

Fig. 6. Ensemble DCNN+DFMI+cGAN Algorithm

The above mentioned ensemble framework explains that the input MRI feature extracted image dataset is taken into DCNN input layer. It generates significant features through convolution layers. These significant features are given into subsampling and classification layer which is processed as output results. After that, the features are given into Conv BN RelU layer and max pooling layer. Then in GAN layer, ANN model is added which is focused to predict and extract more informative features. The efficiency of multiple view image merging is improved by using it. Fig. 6 shows the ensemble DCNN+DFMI+cGAN algorithm

4. Experimental Results

BraTS 2018 is a dataset that offers multi-modal 3D brain MRIs and brain cancer separations interpreted by doctors, that has of 4 MRI modalities for each case (T1, T1c, T2, and FLAIR). Observations contain 3 tumour sub regions - the augmenting tumour, the PeritumoralEdema, and the tumor core, which is necrotic and not improving. Three layered groups of information are created sub-regions – total tumour, central tumour and augmenting tumour. The data are composed from 19 institutes, using numerous MRI scanners. Reliability is one of the effectiveness indicators taken into account, MSE, precision, recall, F-measure and execution time and it is evaluated using existing DCNN,DFMI-Net, TA-cGAN algorithms and proposed ensemble DCNN+DFMI+cGANalgorithm.

Accuracy

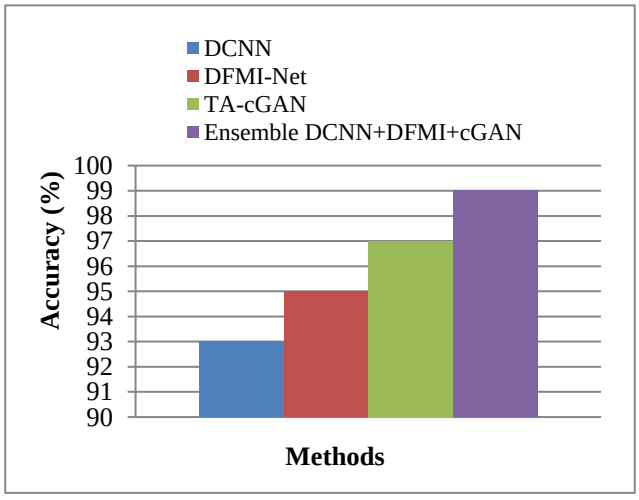

Fig. 7. Accuracy

The comparative metric's correctness is assessed utilizing both the current and suggested methods, as can be seen in the aforementioned Fig. 7. The x-axis is used to represent the techniques, while the y-axis displays the accuracy

value. Among the practices now in use are DCNN, DFMI-Net and TA-cGAN. Although the suggested ensembles of methods offer higher reliability DCNN+DFMI+cGAN for the specified MRI database, method offers improved reliability. The proposed region growing based segmentation algorithm improves image quality via neighbouring pixels. LSOCNN extracts more informative features which increases the image fusion performance. Thus the result concluded that the proposed ensemble DCNN+DFMI+cGAN algorithm increase the overall performance

Precision

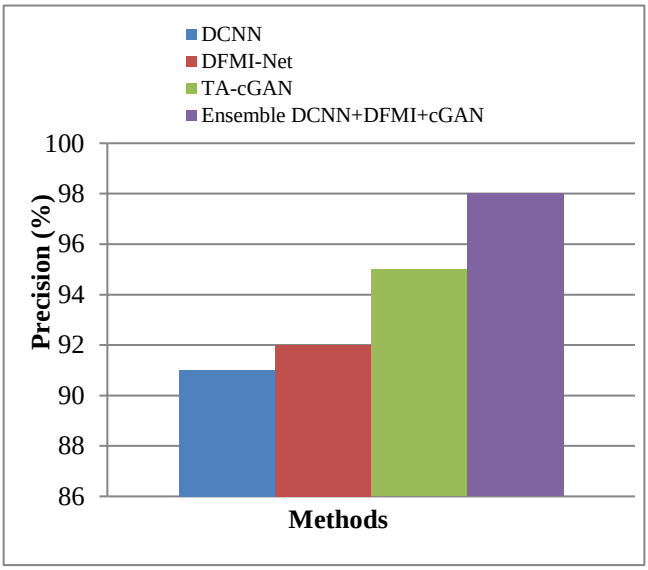

Fig. 8. Precision

The comparative measure is assessed utilizing current methodologies in terms of accuracy, as may been seen in the Fig. 8. Techniques are chosen for the x-axis, and the accuracy values is presented on the y-axis. The proposed ensemble DCNN+DFMI+cGAN method provides higher precision whereas existing DCNN, DFMI-Net and TA-cGAN methods provide lower precision. The goal of the suggested image merging is to create a single, better meaningful image by fusing pertinent data from several MRI views of the same scene. Thus the result concludes that the proposed ensemble DCNN+DFMI+cGAN approach increases the image features accurately for image fusion process. ANN with cGAN the efficiency of the multi view image merging using the best features, according to the algorithm.

Recall

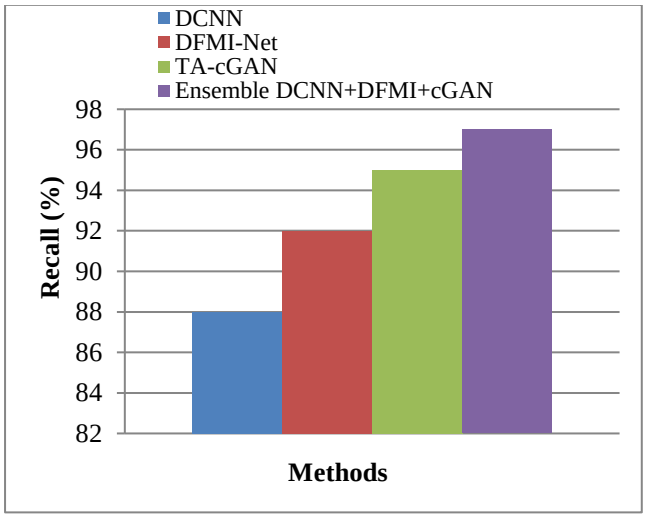

Fig. 9. Recall

The comparative measure is assessed in terms of memory utilizing established methodologies, as can be seen from the aforementioned Fig. 9. The approaches are chosen for the x-axis, and the chart of the recollection values is on the y-axis. The proposed ensemble DCNN+DFMI+cGAN method provides higher recall whereas existing DCNN, DFMI-Net and TA-cGANmethods provide lower recall. RGKMC and LSOCNN algorithm is focused to enhance the quality of the image graph using the best correlated pixels and informative features respectively. The goal of the suggested image merging is to create a single, better meaningful image by fusing pertinent data from several MRI views of the identical subject. Thus the result concludes that the proposed ensemble DCNN+DFMI+cGAN approach increases the image features accurately for image fusion process

F-measure

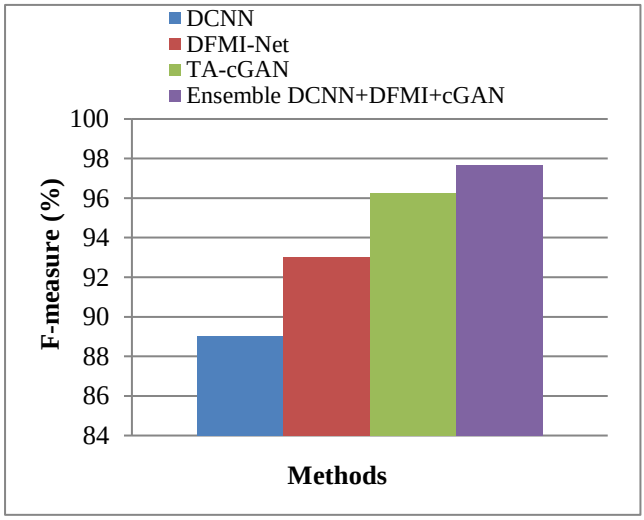

Fig. 10. F-measure

The comparative values of F-measure using existing and proposed algorithms are depicted in Fig. 10. For certain MRI datasets, DCNN, DFMI-Net and existing TA-

methods, cGAN produces lower F-measure values, but the proposed DCNN +DFMI+cGAN classifier ensemble demonstrates an F1 score of 97.7% in prediction with no features being detected wrong. The LSOCNN model is used to extract more informative features that can be used to distinguish between affected and unaffected features. Therefore, the proposed comprehensive deep learning method improves the performance of multi-view image synthesis for MRI databases.

MSE

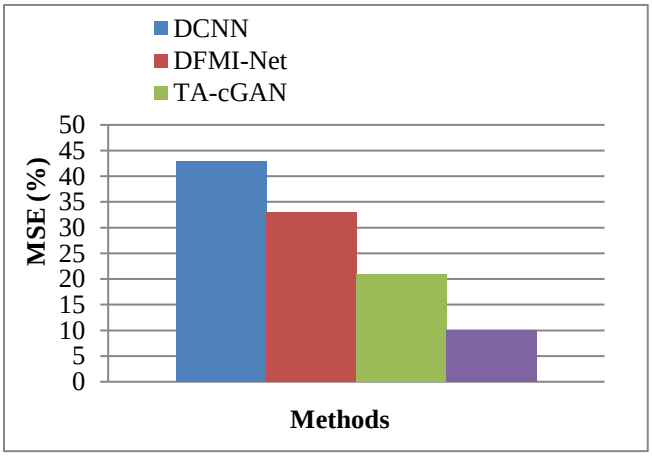

Fig. 11. MSE

As shown in the aforementioned Fig. 11, the comparison measure is assessed in terms of MSE utilizing current methodologies. The approaches are used for the x-axis, and the MSE value is shown on the y-axis. The proposed ensemble DCNN+DFMI+cGAN method provides lower MSE whereas existing DCNN, DFMI-Net and TA-cGAN methods provide higher MSE. The LSOCNN is focused to diminish the errors of multimodal medical image fusions effectively. Thus the result concludes that the proposed ensemble deep learning approach increases the multi view image fusion performance considerably

Execution Time

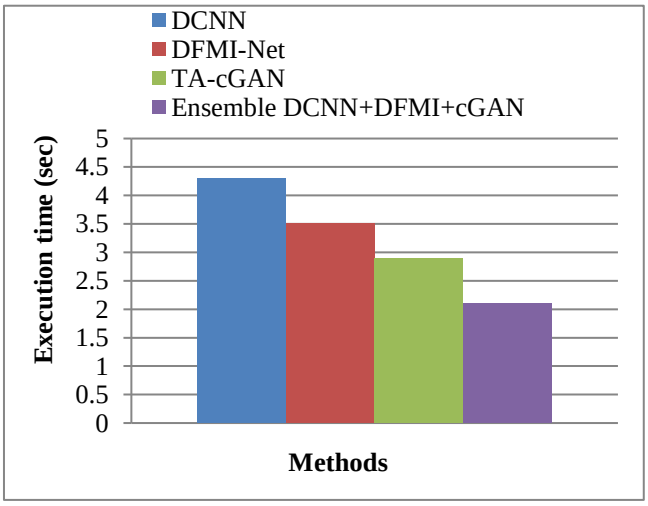

Fig. 12. Execution Time

The comparative measure is assessed utilizing the current and suggested approach in terms of runtime, as could been seen in the aforementioned Fig. 12. In the y-axis, the implementation time values is shown, and the techniques are chosen for the x-axis. The currently used techniques include DCNN, DFMI-Net and TA-cGAN methods provide higher time complexity whereas proposed ensemble DCNN+DFMI+cGAN algorithm provides lower time complexity.The finest pixels are chosen for this suggested study project utilizing RGKMC algorithm and more informative features are extracted via best fitness function values of LSO algorithm. The proposed work increases the speed hence it maximizes the overall image fusion performance. Thus the result concludes that the proposed ensemble deep learning algorithm increase the efficiency

5. Conclusion

In this work, ensemble DCNN+DFMI+cGANa suggested approach merges images for enhanced multi-view performances in the given MRI images. This work is divided into four major modules: noise removal, segmentation, feature extraction, and image fusion. MRI images are segmented using RGKMC algorithm following noise removals to increase image quality. It recognises brain tumours in both black and white images and targets them for prediction. The LSOCNN algorithm is used for feature extraction, which effectively extracts the most informative characteristics. Then the image fusion is performed which fuses the useful and relevant image features which is used for real time applications. The image fusion is done by using ensemble DCNN+DFMI+cGAN algorithm for improving the multi view image fusion performance. In light of the findings of the experiments, it may be deduced that the suggested ensemble DCNN+DFMI+cGAN algorithm provides higher accuracy, precision, recall and lower MSE, execution time rather than the existing algorithm

References

[1] K. Wang, M. Zheng, H. Wei, G. Qi and Y. Li, “Multi-modality medical image fusion using convolutional neural network and contrast pyramid,” *Sensors*, vol. 20, no. 8, pp. 1-17 , 2020.

[2] R. Zhu, X. Li, X. Zhang and M. Ma, “MRI and CT medical image fusion based on synchronized-anisotropic diffusion model,” *IEEE Access*, vol. 8, pp. 91336-91350, 2020.

[3] R. Hou, D. Zhou, R. Nie, D. Liu and X. Ruan, “Brain CT and MRI medical image fusion using convolutional neural networks and a dual-channel

spiking cortical model," *Medical & biological engineering & computing*, vol. 57, pp. 887-900, 2019.

[4] S. Ray, V. Kumar, C. Ahuja and N. Khandelwal, "An automatic method for complete brain matter segmentation from multislice CT scan, " *arXiv preprint arXiv:1809.06215*, pp. 1-17, 2018.

[5] W. Zhao, D. Wang, and H. Lu, "Multi-focus image fusion with a natural enhancement via a joint multi-level deeply supervised convolutional neural network," *IEEE Transactions on Circuits and Systems for Video Technology*, vol. 29, no. 4, pp. 1102-1115, 2018.

[6] M. Bhat and M. V. Karki, "Feature selection based on PCA and PSO for multimodal medical image fusion using DTCWT," *arXiv preprint arXiv:1701.08918*, pp. 1-8, 2017.

[7] J. Chen, X. Li, L. Luo, X. Mei and J. Ma, "Infrared and visible image fusion based on target-enhanced multiscale transform decomposition," *Information Sciences*, vol. 508, pp.64-78, 2020.

[8] V. Subbiah Parvathy, S. Pothiraj and J. Sampson, "A novel approach in multimodality medical image fusion using optimal shearlet and deep learning," *International Journal of Imaging Systems and Technology*, vol. 30, no. 4, pp. 847-859, 2020.

[9] S. L. Hsu, P. W. Gau, I. L. Wu and J. H. Jeng, "Region-based image fusion with artificial neural network," *International Journal of Computer and Information Engineering*, vol. 3, no. 5, pp. 1262-1265, 2009.

[10] Y. Liu, X. Chen, H. Peng and Z. Wang, "Multi-focus image fusion with a deep convolutional neural network," *Information Fusion*, vol. 36, pp. 191-207, 2017.

[11] C. Yan, B. Gong, Y. Wei and Y. Gao, "Deep multi-view enhancement hashing for image retrieval," *IEEE Transactions on Pattern Analysis and Machine Intelligence*, vol. 43, no. 4, pp. 1445-1451, 2020.

[12] J. Ma, H. Xu, J. Jiang, X. Mei and X.P. Zhang, "DDcGAN: A dual-discriminator conditional generative adversarial network for multi-resolution image fusion," *IEEE Transactions on Image Processing*, vol. 29, pp. 4980-4995, 2020.

[13] H. Zhang, Z. Le, Z. Shao, H. Xu and J. Ma, "MFF-GAN: An unsupervised generative adversarial network with adaptive and gradient joint constraints for multi-focus image fusion," *Information Fusion*, vol. 66, pp. 40-53, 2021.

[14] K. Verma, B.K. Singh and A.S. Thoke, "An enhancement in adaptive median filter for edge preservation," *Procedia Computer Science*, 2015, vol. 48, pp. 29-36.

[15] H. Ibrahim, N. S. P. Kong and T. F. Ng, "Simple adaptive median filter for the removal of impulse noise from highly corrupted images," *IEEE Transactions on Consumer Electronics*, vol. 54, no. 4, pp. 1920-19272008..

[16] S. N. Sulaiman, and N. A. M., Isa, "Adaptive fuzzy-K-means clustering algorithm for image segmentation," *IEEE Transactions on Consumer Electronics*, vol. 56, no. 4, pp. 2661-2668, 2010.

[17] A. Javadpour and A. Mohammadi, "Improving brain magnetic resonance image (MRI) segmentation via a novel algorithm based on genetic and regional growth," *Journal of biomedical physics & engineering*, vol. 6, no. 2, pp. 95-108, 2016.

[18] M. Wang, C. Wu, L. Wang, D. Xiang and X. Huang, "A feature selection approach for hyperspectral image based on modified ant lion optimizer," *Knowledge-Based Systems*, vol.168, pp. 39-48, 2019.

[19] H. N. Khan, A. R. Shahid, B. Raza, A. H. Dar and H. Alquhayz, "Multi-view feature fusion based four views model for mammogram classification using convolutional neural network," *IEEE Access*, vol. 7, pp. 165724-165733, 2019.

[20] F. Fan, Y. Huang, L. Wang, X. Xiong, Z. Jiang, Z. Zhang and J. Zhan, "A semantic-based medical image fusion approach," *arXiv preprint arXiv:1906.00225*, pp. 1-6, 2019.

[21] O. Ronneberger, P. Fischer and T. Brox, "U-net: Convolutional networks for biomedical image segmentation," *Medical Image Computing and Computer-Assisted Intervention–MICCAI 2015: 18th International Conference, Munich, Germany, October 5-9, 2015, Proceedings, Part III 18*, pp. 234-241.

[22] J. Ting, K. Punithakumar and N. Ray, "Multiview 3-d echocardiography image fusion with mutual information neural estimation," *IEEE International Conference on Bioinformatics and Biomedicine (BIBM), December 2020*, pp. 765-771.

[23] Y. Wang, B. Yu, L. Wang, C. Zu, D. S. Lalush, W. Lin, X. Wu, J. Zhou, D. Shen and L. Zhou, "3D conditional generative adversarial networks for high-quality PET image estimation at low dose," *Neuroimage*, vol. 174, pp. 550-562, 2018.

[24] I. Goodfellow, J. Pouget-Abadie, M. Mirza, B. Xu, D. Warde-Farley, S. Ozair and Y. Bengio, "Generative

adversarial networks," *Communications of the ACM*, vol. 63, no. 11, pp. 139-144, 2020.

[25] J. Kang, W. Lu and W. Zhang, "Fusion of brain PET and MRI images using tissue-aware conditional generative adversarial network with joint loss," *IEEE Access*, vol. 8, pp. 6368-6378, 2020.

[26] N. E. K. Mohamed and A. S. M. El-Bhrawy, "Artificial neural networks in data mining," *IOSR Journal of Computer Engineering*, vol. 18, pp. 55-59, 2016.

[27] M. A. Parwez and M. Abulaish, "Multi-label classification of microblogging texts using convolution neural network," *IEEE Access*, vol. 7, pp. 68678-68691, 2019.

[28] M. Yaseen, H. S. Salih, M. Aljanabi, A. H. Ali and S. A. Abed, "Improving Process Efficiency in Iraqi universities: a proposed management information system," *Iraqi Journal For Computer Science and Mathematics*, vol. 4, no. 1, pp. 211-219, 2023.

[29] M. Aljanabi and S. Y. Mohammed, "Metaverse: open possibilities," *Iraqi Journal For Computer Science and Mathematics*, vol. 4, no. 3, pp. 79-86, 2023.

[30] A. S. Shaker, O. F. Youssif, M. Aljanabi, Z. Abbood and M.S. Mahdi, "SEEK Mobility Adaptive Protocol Destination Seeker Media Access Control Protocol for Mobile WSNs," *Iraqi Journal For Computer Science and Mathematics*, vol. 4, no. 1, pp. 130-145, 2023.

[31] H. S. Salih, M. Ghazi and M. Aljanabi, "Implementing an Automated Inventory Management System for Small and Medium-sized Enterprises," *Iraqi Journal For Computer Science and Mathematics*, vol. 4, no. 2, pp. 238-244, 2023.